



Influence of metal oxides on Pt catalysts for methanol electrooxidation using electrochemical impedance spectroscopy

Huiping Yuan^{a,b}, Daojun Guo^a, Xinping Qiu^{a,b,*}, Wentao Zhu^a, Liquan Chen^{a,b}

^a Key Laboratory of Organic Optoelectronics and Molecular Engineering, Department of Chemistry, Tsinghua University, Beijing 100084, China

^b Lab of Advanced Power Sources, Graduate School at Shenzhen, Tsinghua University, Shenzhen 518055, China

ARTICLE INFO

Article history:

Received 19 November 2008

Accepted 25 November 2008

Available online 3 December 2008

Keywords:

Electrochemical impedance

Metal oxide

Methanol electrooxidation

Direct methanol fuel cell

ABSTRACT

Carbon nanotubes used as supports for platinum catalysts deposited with metal oxides (CeO₂, TiO₂, and SnO₂) were prepared for their application as anode catalysts in a direct methanol fuel cell. Cyclic voltammetry, chronoamperometry, and electrochemical impedance spectroscopy measurements were carried out in a solution of 0.5 M CH₃OH and 0.5 M H₂SO₄. Catalysts with the addition of CeO₂, TiO₂, and SnO₂ presented higher catalytic activity than pure platinum catalysts, and the catalysts with CeO₂ were the best among them. Electrochemical impedance spectra indicated that methanol electrooxidation on these catalysts had different impedance behaviors at different potential regions. The mechanism of methanol electrooxidation changed with increases of the potential. The promotion effect of the metal oxides lies in the oxidation of intermediate CO_{ads} on Pt at low potential regions.

© 2009 Published by Elsevier B.V.

1. Introduction

Fuel cells, due to their high theoretical fuel efficiency and low environmental impact, have been paid much attention to in recent years [1,2,21]. The fuel cell is the most promising power source for automotive, portable, and stationary applications. Although hydrogen is an ideal fuel for polymer electrolyte membrane fuel cells (PEMFC), it is very dangerous to store it under high pressure. The production of hydrogen is still problematic. To avoid these disadvantages, the direct methanol fuel cell (DMFC) has been developed with a simplified structural system, using aqueous methanol as the fuel. But the high cost and low activity of Pt catalysts for methanol oxidation limit the commercialization of DMFC.

It is widely accepted that CO species produced in the process of methanol electrooxidation are the main poisoning intermediate that slows down the oxidation kinetics. For resolving this problem, Pt-based binary catalysts (PtRu [3,4], PtMo [5,6], PtSn [7,8], etc.) and ternary catalysts (PtRuMo [9], PtRuNi [10], etc.) have been studied to improve the catalytic activity of Pt through bifunctional mechanism or electronic effects. Besides this, it has been found that directly added elements in oxidation states [11] or metal oxides (TiO₂ [12],

ZrO₂ [13], MoO₂ [14], etc.) can effectively promote the electrooxidation of methanol and show perfect tolerance to CO poisoning. First, metal oxides stabilize Pt particle dispersion, being in favor of the increase of active surface per weight of the catalyst. Second, they possess a good capacity for storing and releasing oxygen, which plays an important role in CO_{ads} electrooxidation. At the same time, the low price and the abundance of metal oxides can help reduce the cost of DMFC. Therefore, they are promising additives for Pt catalysts.

However, metal oxides have one drawback: their low electrical conductivity, which affects the catalytic activity of Pt. In this research, carbon nanotubes (CNTs) were used as the support which provided a large network for collecting electrons from the oxidation process, thereby assisting efficient current generation. Metal oxides (CeO₂, TiO₂ and SnO₂) and Pt nanoparticles were successively deposited on carbon nanotubes. The influence of metal oxides on the catalytic activity of Pt for electrooxidation of methanol has been tested by cyclic voltammetry (CV), chronoamperometry, and electrochemical impedance spectroscopy (EIS) methods, aiming to determine the most promising catalyst application in fuel cells. In addition, the EIS technique is a good tool for analyzing the kinetics of electrode reactions. The component in the circuit has a clear physical significance related to the reaction mechanism. Although, there have been many electrochemical impedance investigations of methanol electrooxidation on Pt electrodes [15–19], EIS influenced by metal oxides has not been reported. Herein, we preliminarily discuss the mechanisms of different catalysts using EIS.

* Corresponding author at: Key Laboratory of Organic Optoelectronics and Molecular Engineering, Department of Chemistry, Tsinghua University, Beijing 100084, China. Tel.: +86 10 62794234 fax: +86 10 62794234.

E-mail address: qiuxp@mail.tsinghua.edu.cn (X. Qiu).

2. Experimental

2.1. Preparation of catalysts

Multi-walled carbon nanotubes (MWCNTs) were obtained from the Chemical Engineering Department of Tsinghua University. The as-received MWCNTs were dipped in HCl solution for 2 days, and then refluxed in a solution of 3 M H_2SO_4 and 3 M HNO_3 at 70°C for 48 h. A TiO_2/CNT substrate was prepared by the sol-gel method using tetrabutyl titanate as the precursor, ethanol as the solvent, and acetic acid as the stabilizer. The functionalized CNTs were put into the sol, stirred for 20 min, and dried at 80°C in an oil bath. CeO_2/CNT and SnO_2/CNT substrates were prepared through the precipitation method. First, a $\text{Ce}(\text{NO}_3)_3$ or an SnCl_4 solution containing CNTs was ultrasonically mixed. Then ammonia solution was dropwise added into the solution until the pH was 7. The solution was stirred for 2 h, filtered, and dried.

Pt nanoparticles were generated by microwave heating of an ethylene glycol solution of Pt precursor salts [20]. An ethylene glycol solution containing 0.06 M NaOH and 0.2 M H_2PtCl_6 was placed in the center of a microwave oven (Glanz brand microwave 750 W) and heated for 60 s. Then this solution was added to an aqueous suspension of MO_2/CNT ($\text{M} = \text{Ce}, \text{Ti}, \text{Sn}$) or CNT substrates and stirred for 4 h. After 4 h of adsorption of Pt nanoparticles, the suspension was filtered, washed with deionized water, and dried at 80°C . The loading of Pt nanoparticles was 20 wt%. The molar ratio of Pt and metal oxide of $\text{Pt}/\text{MO}_2/\text{CNT}$ catalyst was 1:3.

2.2. Electrochemical measurements

A solution of 25 μL Nafion solution (20% Nafion and 80% ethylene glycol) and 75 μL H_2O containing 1 mg of the catalyst was ultrasonically dispersed for 30 min. Then the suspension was cast onto the surface of a polished Au electrode (1 cm^2) and dried at 80°C for 45 min. Electrochemical measurements were carried out on a PAR-STAT 2273 workstation. A conventional three-electrode cell, with Pt foil as the counter electrode, and with a saturated calomel electrode (SCE) as the reference electrode, was used. The electrochemical measurements were carried out at 20°C . All potentials reported in this article are with respect to SCE.

Before each measurement, the electrolyte was purged with N_2 gas for 20 min to remove the dissolved oxygen, and the electrode was performed with an electrochemical cleaning by scanning the potential between -0.2 and 1.0 V vs. SCE with a sweep rate of 50 mV s^{-1} . The electrooxidation of methanol was carried out in a solution of $0.5\text{ M H}_2\text{SO}_4 + 0.5\text{ M CH}_3\text{OH}$ at a sweep rate of 50 mV s^{-1} . The real surface area of Pt was calculated with a cyclic voltammogram assuming $210\text{ }\mu\text{C cm}^{-2}$ per monolayer adsorbed H. The current density was relative to a square centimeter of Pt. The impedance spectra were registered at frequencies from 100 kHz to 100 mHz with a logarithmic data collection of 15 points per decade. A sine wave of 10 mV amplitude at the desired potential was applied. ZSimpWin software was used to analyze the impedance data.

3. Results and discussion

Typical cyclic voltammograms of Pt/CNT, Pt/ CeO_2/CNT , Pt/ TiO_2/CNT and Pt/ SnO_2/CNT catalysts in $0.5\text{ M H}_2\text{SO}_4$ are shown in Fig. 1. Pt surface areas, estimated from hydrogen desorption and adsorption peaks, are approximately the same for different catalysts. While in the oxygen adsorption and desorption region, all the catalysts with metal oxides exhibit higher current density to a different degree than Pt/CNTs. This suggests that metal oxides may offer oxygen-containing species which promote the adsorption of oxygen on Pt.

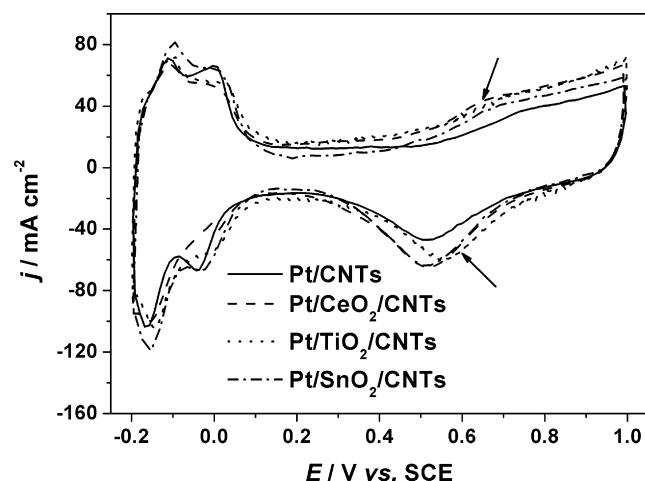


Fig. 1. The cyclic voltammograms of Pt/CNT, Pt/ CeO_2/CNT , Pt/ TiO_2/CNT and Pt/ SnO_2/CNT catalysts in $0.5\text{ M H}_2\text{SO}_4$; $\nu = 50\text{ mV s}^{-1}$.

Fig. 2 presents the typical cyclic voltammograms of Pt/CNT and different Pt/ MO_2/CNT ($\text{M} = \text{Ce}, \text{Ti}, \text{Sn}$) catalysts toward methanol oxidation in $0.5\text{ M H}_2\text{SO}_4 + 0.5\text{ M CH}_3\text{OH}$ solution at 50 mV s^{-1} . The onset oxidation potential of the positive scan is at 0.47 V vs. SCE and the oxidation peak current density is 0.4 mA cm^{-2} on the Pt/CNT electrode. The presence of metal oxides makes the onset potential shift negatively. As shown in the insert in Fig. 2, different oxides show different onset potentials for methanol oxidation: 0.37 V for Pt/ CeO_2/CNT s, 0.39 V for Pt/ TiO_2/CNT s, and 0.42 V for Pt/ SnO_2/CNT s. The onset potential for methanol oxidation is a determining element in evaluating the activity of an electrode. Therefore, the catalytic activity of the electrode was promoted by adding metal oxides. The oxidation peak current densities also had increases of different degrees. They were 0.87 , 0.55 , and 0.43 mA cm^{-2} for the Pt/ CeO_2/CNT , Pt/ TiO_2/CNT , and Pt/ SnO_2/CNT catalysts, respectively.

The performance of Pt/ MO_2/CNT catalysts compared to Pt/CNTs was also tested by the chronoamperometry method. The short-time current density at a constant potential of 0.4 V in $0.5\text{ M H}_2\text{SO}_4 + 0.5\text{ M CH}_3\text{OH}$ solution is shown in Fig. 3. Similar to the CV results, the Pt/ CeO_2/CNT catalyst still demonstrates the highest current density of 0.2 mA cm^{-2} . The current densities of the Pt/ TiO_2/CNT and Pt/ SnO_2/CNT catalysts were lower, with values of 0.1 and 0.05 mA cm^{-2} , respectively. It is generally thought that the addition of a second metal or metal oxide to Pt catalysts signifi-

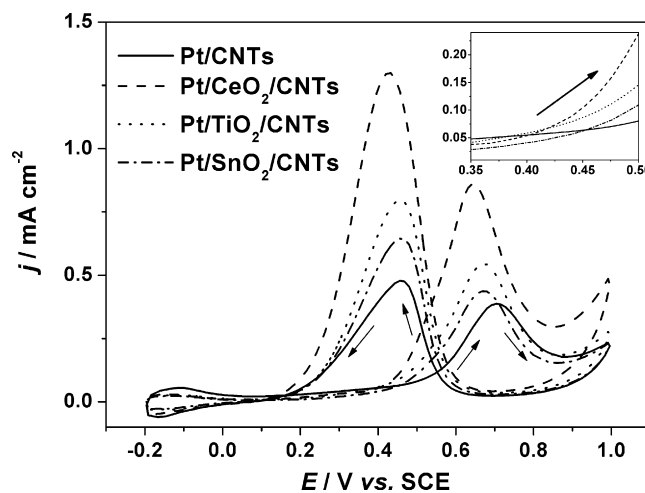


Fig. 2. The cyclic voltammograms of methanol electrooxidation in $0.5\text{ M H}_2\text{SO}_4 + 0.5\text{ M CH}_3\text{OH}$ solution; $\nu = 50\text{ mV s}^{-1}$.

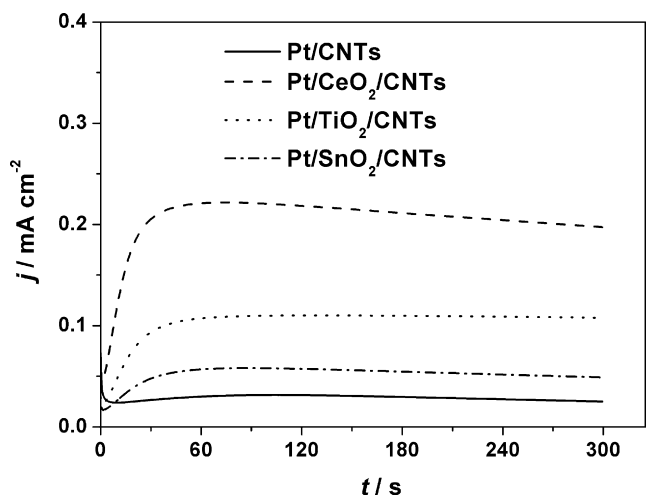


Fig. 3. Chronoamperometric curves at 0.4 V vs. SCE in 0.5 M H₂SO₄ + 0.5 M CH₃OH solution.

cantly decreases the overpotential of a methanol electrooxidation reaction through a bifunctional mechanism, according to which oxygen-containing species necessary for the oxidation of intermediates of methanol dehydrogenation can be generated under lower potential on the added metal. In our experiment, different metal oxides exhibited the distinct influence on methanol electrooxidation. We consider this to have been due to the different surface characters of metal oxides.

Electrochemical impedance is a powerful technique for investigating the kinetics of small organic molecules' electrooxidation in fuel cells [21–24]. As can be seen from the above results, the loading of metal oxides can effectively enhance the activity of methanol electrooxidation. The purpose of employing impedance spectra is to obtain the electrocatalytic activity in terms of charge-transfer resistance. Electrochemical impedance measurements of the Pt/CNT and Pt/MO₂/CNT (M = Ce, Ti, Sn) catalysts at various potentials, from 0.05 to 0.9 V, were performed in a 0.5 M H₂SO₄ + 0.5 M CH₃OH solution. The complex-plane plots are presented in Figs. 4–7. The reaction of methanol electrooxidation contains one adsorbed intermediate. The impedance data were fitted using the equivalent circuits shown in Fig. 8. Fig. 8a depicts the equivalent circuit for the impedance spectra without pseudo-inductive behavior, where R_s is the solution resistance, R_{ct} is the charge-transfer resistance, and the constant-phase element CPE₂ is the electric double-layer capacitance used instead of a capacitor to account for the porous catalysts. A parallel constant-phase element (CPE₁) and resistor (R_e) were added in series to fit the high frequency impedance data, which were attributed to a charge-transfer process at the outermost surface of the electrode [18]. The equivalent circuit in Fig. 8b was used for modeling the pseudo-inductive impedance, where R_L and L were the resistance and inductance of the adsorbed layer. The fit based on the modified equivalent circuit agreed well with the experimental data throughout the whole frequency range studied.

Charge-transfer resistances presented negative values, between 0.45 and 0.65 V, when the impedance spectra reversed to the second quadrant. At potentials higher than 0.7 V, the values of R_{ct} of different catalysts were approximately the same. The charge-transfer resistances of Pt/MO₂/CNT electrodes, compared with Pt/CNTs at electrode potentials from 0.05 to 0.45 V, are shown in Fig. 9. The impedance spectra exhibited four potential regions, where there were changes in the mechanism for methanol electrooxidation, between 0.05 and 0.9 V.

At potentials below 0.2 V, on the Pt/CNT electrode, the diameter of the impedance arc and the fitted charge-transfer resistance were almost unchanged from increasing the electrode potential.

The potential was too low for water dissociation to form OH_{ads}, and the Pt surface was inactivated. This was attributed to the largely covered CO_{ads} generated from methanol dehydrogenation. Between 0.2 and 0.4 V, the diameter of the arc began to decrease. As shown in Fig. 9, the charge-transfer resistance decreased exponentially, with a Tafel slope of 116 mV per decade, which accords well with the Tafel slope reported previously [17]. This indicates that the rate-limiting step is a one electron process and the oxidation removal of the adsorbed poisoning species CO starts to occur.

When metal oxides were loaded, the charge-transfer resistance began to decrease at a much lower potential than Pt/CNTs. The accumulation process of intermediate CO_{ads}, which blocks incessant adsorption and dehydrogenation of methanol, was not observed as it was on the Pt/CNT electrode. The oxygen-containing species participating in CO_{ads} oxidation are mainly afforded by metal oxides. The initial decrease rate of the charge-transfer resistance depended on the category of metal oxides. It was faster on Pt/CeO₂/CNTs than on Pt/TiO₂/CNTs, and was the smallest on Pt/SnO₂/CNTs. The order of the decrease rate was consistent with the onset potential and current density of methanol oxidation, as shown in the insert in Fig. 2. Comparing the values of R_{ct} of the catalysts at potentials below 0.2 V, the order was Pt/SnO₂/CNTs < Pt/TiO₂/CNTs < Pt/CeO₂/CNTs, which was in the

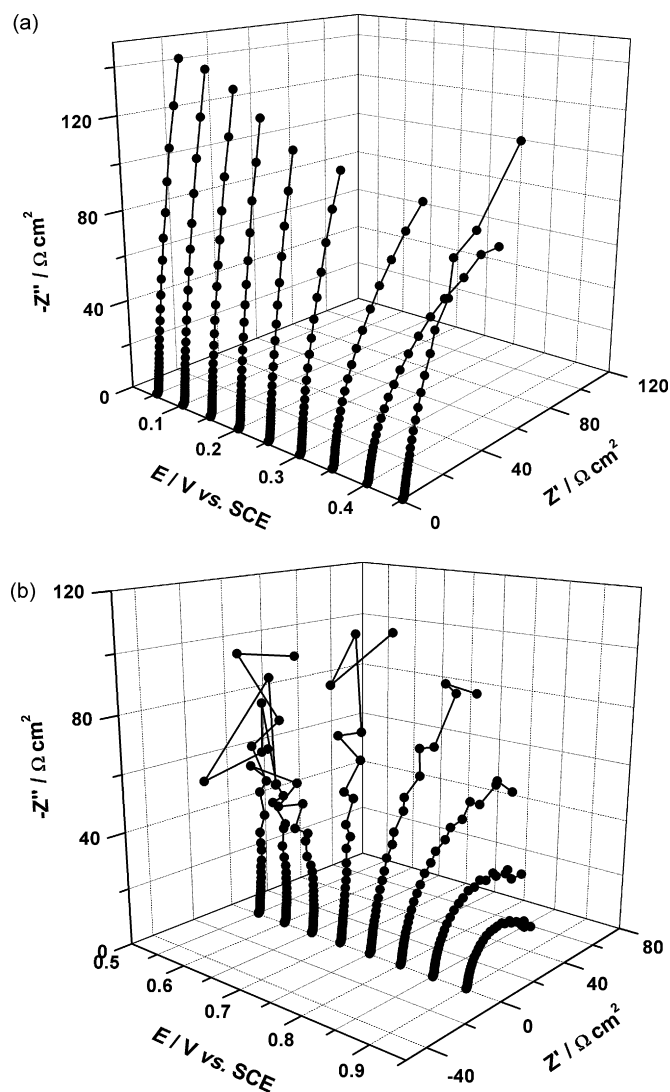


Fig. 4. Complex-plane impedance plots of Pt/CNTs in 0.5 M H₂SO₄ + 0.5 M CH₃OH solution at various electrode potentials.

opposite direction of the electrical conductivity of the metal oxides ($\text{CeO}_2 < \text{TiO}_2 < \text{SnO}_2$). In the low potential region, methanol dehydrogenation was the dominant reaction. Although CO_{ads} oxidation occurred on the Pt/ MO_2 /CNT electrode, the reaction rate was very slow. The influence of low electrical conductivity of the metal oxides was comparatively significant.

With the potential increasing, Tafel slopes were also observed on Pt/ MO_2 /CNT electrodes, which indicated the same reaction mechanism with the Pt/CNT electrode. The charge-transfer resistances were much smaller on the Pt/ CeO_2 /CNT and Pt/ TiO_2 /CNT electrodes, and typical pseudo-inductive behavior was present in the fourth quadrant in the impedance plots. Generally, pseudo-inductive behavior is attributed to the oxidation of the CO_{ads} coverage layer, while the subsequent methanol oxidation taking place within the empty holes [16,18]. This meant that the Pt surface was gradually cleaned up and the oxidation rate was accelerated. Whereas the values of R_{ct} on Pt/ SnO_2 /CNT electrode were almost the same as that for the Pt/CNT electrode, this does not suggest an obvious advantage in reaction activity.

At potentials between 0.4 and 0.6 V, the diameter of the arc increased at first; then, the arc reversed to the second quadrant.

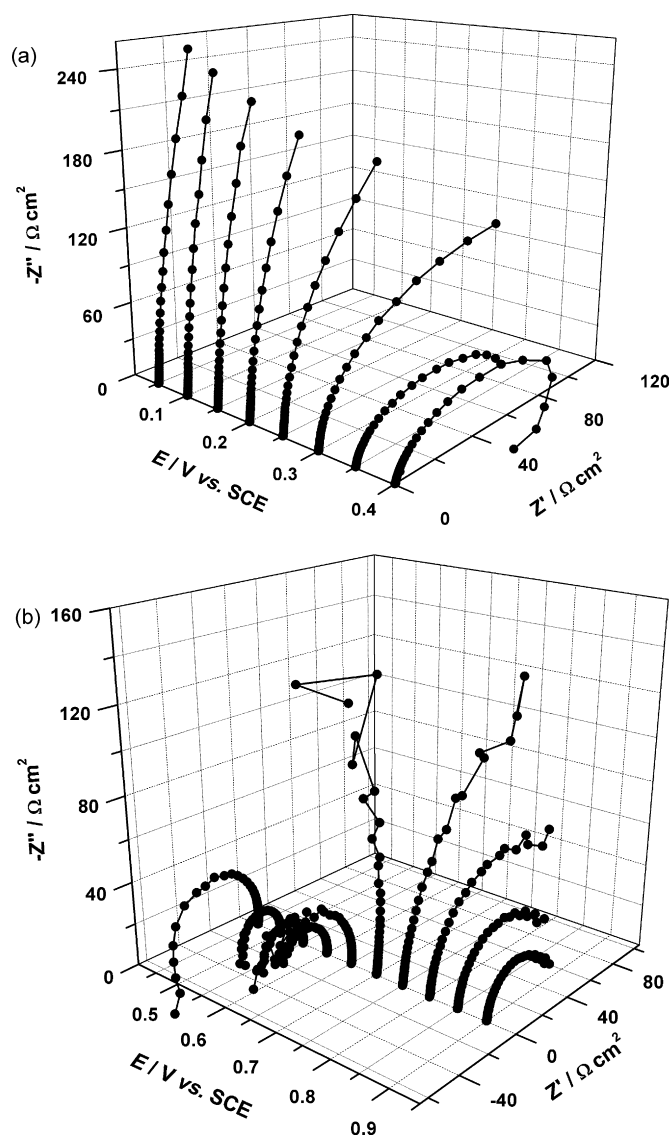


Fig. 5. Complex-plane impedance plots of Pt/ CeO_2 /CNTs in $0.5 \text{ M H}_2\text{SO}_4 + 0.5 \text{ CH}_3\text{OH}$ solution at various electrode potentials.

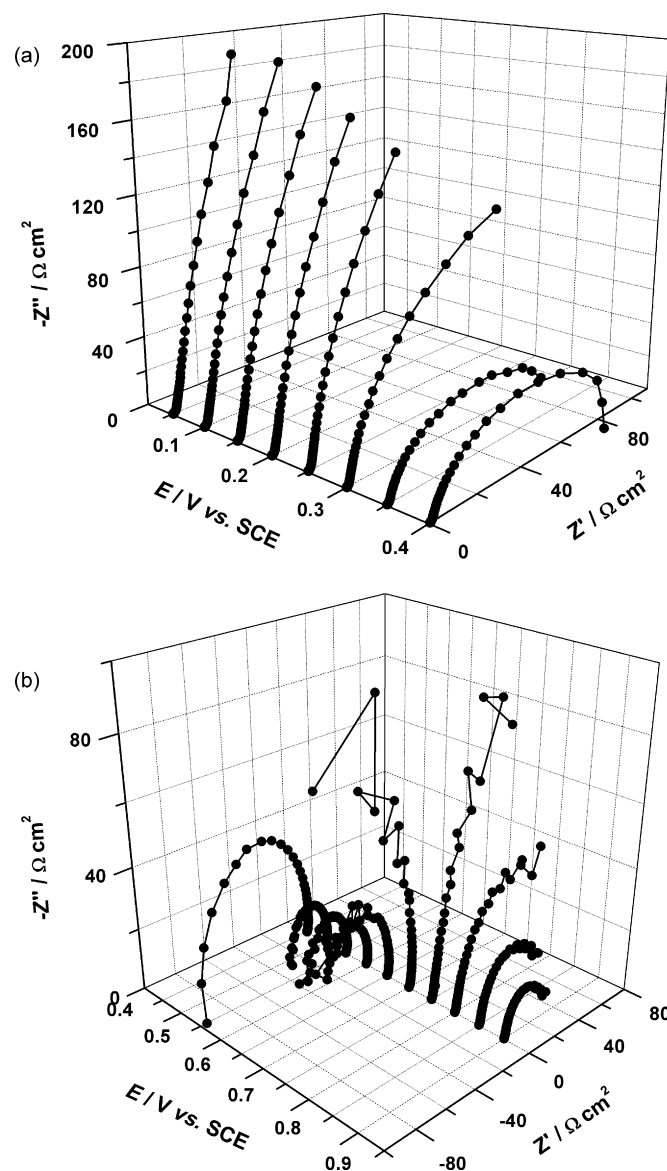


Fig. 6. Complex-plane impedance plots of Pt/ TiO_2 /CNTs in $0.5 \text{ M H}_2\text{SO}_4 + 0.5 \text{ CH}_3\text{OH}$ solution at various electrode potentials.

With further increases of the potential, the arc diameter decreased. The reverse behavior reported previously has been explained by the effect of the largely formed chemisorbed hydroxyl groups, which enhance the oxidation of the adsorbed intermediates and block the sites of methanol adsorption. On Pt/ CeO_2 /CNT and Pt/ TiO_2 /CNT electrodes, the impedance plots still exhibited a pseudo-inductive arc in the third quadrant, indicating that the methanol oxidation reaction was faster than for the Pt/CNT and Pt/ SnO_2 /CNT electrodes.

From 0.6 V to higher potentials, the diameter of the arc increased with electrode potential until, at 0.7 V, the impedance arc flipped back to the first quadrant. The arc diameter and the charge-transfer resistance decreased with further increases in electrode potential. In this potential region, the platinum surface was entirely covered by hydroxyl groups, inhibiting the oxidation of methanol. The charge-transfer resistances of different catalysts at various potentials were equivalent.

Based on the above analysis, the electrochemical impedance performances of Pt/ CeO_2 /CNT and Pt/ TiO_2 /CNT catalysts are similar. Their catalytic activities are higher than Pt/ SnO_2 /CNT catalysts

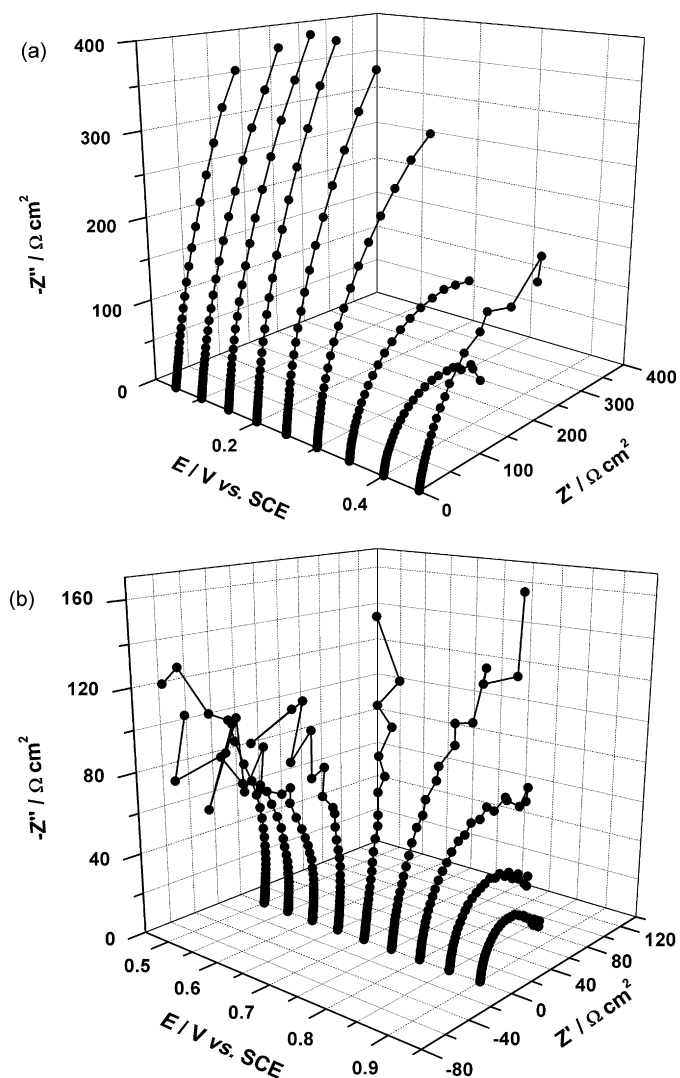


Fig. 7. Complex-plane impedance plots of Pt/SnO₂/CNTs in 0.5 M H₂SO₄ + 0.5 CH₃OH solution at various electrode potentials.

which are approximately the same as Pt/CNT catalysts. This accords well with CV and chronoamperometric data. The most remarkable effect from adding metal oxides were present at the low potential region from 0.05 to 0.4 V. Charge-transfer resistance began to decrease, which represented the oxidation of CO_{ads}, at lower potentials than pure Pt. Hence the subsequent oxidation rate sped up.

We think the promotion effect operated through a bifunctional mechanism: hydroxyl groups on the surface of metal oxides can be greatly generated by the dissociation of coordinated water

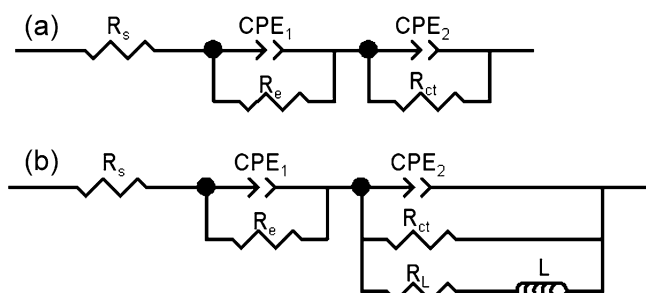


Fig. 8. Equivalent circuits for modeling the impedance spectra.

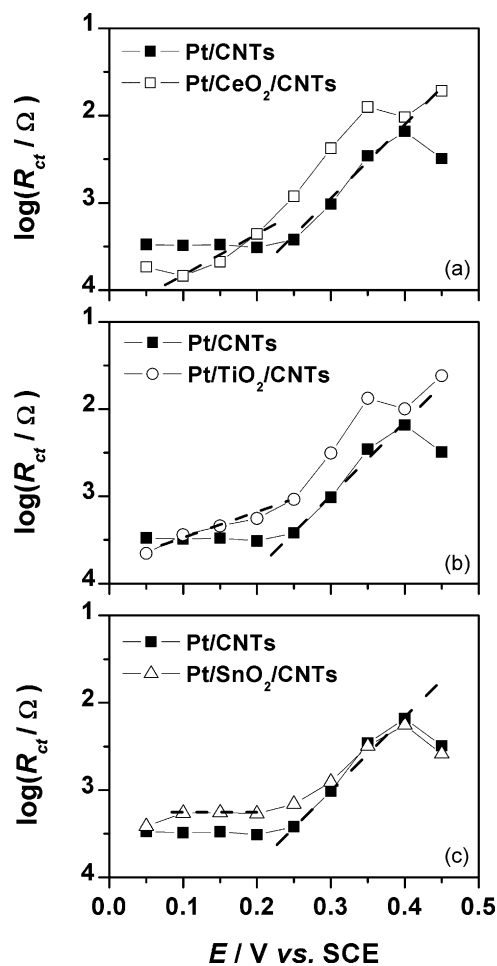


Fig. 9. The charge-transfer resistance of methanol electrooxidation as a function of the electrode potential.

molecules. However, various metal oxides exhibit the distinguishing electrochemical impedance behaviors. Note, for example, the different decrease rates of charge-transfer resistance at potentials lower than 0.2 V. We suggest that this is attributable to the intrinsic properties of metal oxides, including the density of surface hydroxyl groups and the reaction activation energy of CO_{ads} with OH_{ads} on metal oxides. These problems need to be further studied using in situ spectral electrochemical methods.

4. Conclusions

In this paper, different Pt/MO₂/CNT catalysts (M = Ce, Ti, Sn) were prepared and the electrocatalytic performances in respect to the electrooxidation of methanol in H₂SO₄ solution were investigated. The cyclic voltammograms showed that the onset potential of methanol oxidation shifts negatively and that the current density of the oxidation peak increases, compared to Pt/CNT catalysts. Pt/CeO₂/CNTs exhibited the highest catalytic activity in the catalysts investigated. The kinetics of methanol oxidation were studied using electrochemical impedance spectra. It was found that metal oxides can promote the electrooxidation of CO_{ads}, which was demonstrated by a decrease of the charge-transfer resistance at a low potential region. The accumulation process of CO_{ads} was not observed as it was on the Pt/CNT electrode. In addition, the decreased rate of charge-transfer resistance was determined by the metal oxides added, which indicated different reaction activity of CO_{ads} oxidation with hydroxyl groups on various metal oxides.

Acknowledgments

This work was supported by the State Key Basic Research Program of PRC (2009CB220105) and Beijing National Science Foundation (2071001).

References

- [1] Y.Y. Shao, G.P. Yin, Y.Z. Gao, J. Power Sources 171 (2007) 558–566.
- [2] J.H. Wee, K.Y. Lee, S.H. Kim, J. Power Sources 165 (2007) 667–677.
- [3] M.T.M. Koper, J.J. Lukkien, A.P.J. Jansen, R.A. van Santen, J. Phys. Chem. B 103 (1999) 5522–5529.
- [4] Q.Y. Lu, B. Yang, L. Zhuang, J.T. Lu, J. Phys. Chem. B 109 (2005) 1715–1722.
- [5] A.E. Russell, S.C. Ball, S. Maniguet, D. Thompsett, J. Power Sources 171 (2007) 72–78.
- [6] J.G. Wang, B. Hammer, J. Catal. 243 (2006) 192–198.
- [7] Y.L. Guo, Y.Z. Zheng, M.H. Huang, Electrochim. Acta 53 (2008) 3102–3108.
- [8] Z. Liu, D. Reed, G. Kwon, M. Shamsuzzoha, D.E. Nikles, J. Phys. Chem. C 111 (2007) 14223–14229.
- [9] D.A. Stevens, J.M. Rouleau, R.E. Mar, R.T. Atanasoski, A.K. Schmoekkel, M.K. Debe, J.R. Dahn, J. Electrochem. Soc. 154 (2007) 1211–1219.
- [10] B. Moreno, E. Chinarro, J.C. Perez, J.R. Jurado, Appl. Catal. B 76 (2007) 368–374.
- [11] D.R. Rolison, P.L. Hagans, K.E. Swider, J.W. Long, Langmuir 15 (1999) 774–779.
- [12] H.Q. Song, X.P. Qiu, D.J. Guo, F.S. Li, J. Power Sources 178 (2008) 97–102.
- [13] N.F.P. Ribeiro, F.M.T. Mendes, C.A.C. Perez, M.M.V.M. Souza, M. Schmal, Appl. Catal. A 347 (2008) 62–71.
- [14] T. Ioroi, T. Akita, S. Yamazaki, Z. Siroma, N. Fujiwara, K. Yasuda, Electrochim. Acta 52 (2006) 491–498.
- [15] J.T. Muller, P.M. Urban, W.F. Holderich, J. Power Sources 84 (1999) 157–160.
- [16] R.E. Melnick, G.T.R. Palmore, J. Phys. Chem. B 105 (2001) 1012–1025.
- [17] F. Seland, R. Tunold, D.A. Harrington, Electrochim. Acta 51 (2006) 3827–3840.
- [18] W. Sugimoto, K. Aoyama, T. Kawaguchi, Y. Murakami, Y. Takasu, J. Electroanal. Chem. 576 (2005) 215–221.
- [19] I.M. Hsing, X. Wang, Y.J. Leng, J. Electrochem. Soc. 149 (2002) A615–A621.
- [20] Z.L. Liu, J.Y. Lee, W.X. Chen, M. Han, L.M. Gan, Langmuir 20 (2004) 181–187.
- [21] P. Bommersbach, M. Mohamedi, D. Guay, J. Electrochem. Soc. 154 (2007) B876–B882.
- [22] Z.B. Wang, G.P. Yin, Y.Y. Shao, B.Q. Yang, P.F. Shi, P.X. Feng, J. Power Sources 165 (2007) 9–15.
- [23] W. Chen, J. Kim, L. Xu, S. Sun, S. Chen, J. Phys. Chem. C 111 (2007) 13452–13459.
- [24] A.L. Ocampo, M. Miranda-Hernandez, J. Morgado, J.A. Montoya, P.J. Sebastian, J. Power Sources 160 (2006) 915–924.